Master's thesis

NTNU
Norwegian University of Science and Technology
Faculty of Engineering
Department of Geoscience and Petroleum

Bård Torarin Sandahl

Inducing Latereal Drillstring Movements to Improve Hole Cleaning

Master's thesis in Petroleum Engineering
Supervisor: Sigve Hovda
June 2020

NTNU
Norwegian University of
Science and Technology

Bård Torarin Sandahl

Inducing Latereal Drillstring Movements to Improve Hole Cleaning

Master's thesis in Petroleum Engineering
Supervisor: Sigve Hovda
June 2020

Norwegian University of Science and Technology
Faculty of Engineering
Department of Geoscience and Petroleum

NTNU
Norwegian University of
Science and Technology

Abstract

Drillstring rotation is a well-known method of improving hole cleaning in deviated wells. In this thesis, the hole cleaning effects of drawworks induced lateral drillstring movements have been investigated both as a stand alone method, and in combination with drillstring rotation. These induced lateral drillstring movements have been dubbed drillstring slamming. The concept of drillstring slamming is to rapidly change the drillstring eccentricity in the wellbore in order to create jet flows via piston displacement of the fluid in the annular space. This acceleration of fluid in combination with the drillstring impacting the cuttings bed is hypothesized to aid in dislodging and suspending cuttings from the cuttings bed. In order to investigate its potential, an existing flow loop at the Deparment of Geoscience and Petroleum at NTNU was modified. The primary focus of these modifications was to improve the repeatability of experiments conducted on this flow loop rig. In part, the objective of the work documented in this thesis has been to verify the effect of these modifications.

In order to understand the effects of drillstring slamming, the hole cleaning performance at 60° inclination have been investigated for annular flow alone, drillstring rotation, drillstring slamming and drillstring rotation in combination with drillstring slamming. The experiments were conducted using tap water, and repeated using a xanthan gum fluid to investigate the effect of viscosity on hole cleaning performance at this inclination.

It was observed that the flow loop design changes significantly improved the repeatability of experiments. Drillstring slamming was found to be far less effective than drillstring rotation using the xanthan gum fluid. However, drillstring slamming seems to be more effective than annular flow alone, and there was found no indication that slamming negates the effects of drillstring rotation. The tests using tap water indicated that annular flow rate and drillstring eccentricity dominate the hole cleaning performance when circulating low viscosity fluids.

Acknowledgement

I would like thank my supervisor, Sigve Hovda, for his inputs on how to structure a thesis. I would also like to thank him for his continued interest in this project, and his many motivational talks and suggestions. I would also like to thank Noralf Vedvik and Steffen Wærnes Moen for their assistance in acquiring the necessary parts for the redesign of the flow loop, as well as their contribution to the assembly of the setup. I would like to thank Titus Ntow Ofei for suggesting the use glycerol, although it did not come to be. Finally, I would like to thank my good friend and fellow student, Christoffer Schjem Sørgård, for his contribution to the fluid selection process and associated collaborative work.

Table of Contents

List of Tables

List of Figures

Chapter 1

Introduction

Oil wells are constructed to create a path for hydrocarbons to flow from the reservoir to the surface. An oil well is constructed by drilling. The drill bit is driven into the ground by applying weight and rotating the bit. The drill bit is connected to the drilling rig via drillpipe. As the drill bit penetrates the rock, cuttings are generated. Cuttings are rock fragments that break off as the drill bit progresses through the rock. These cuttings have to be continuously removed in order for drilling to progress. Cuttings are removed by pumping a fluid, often called drilling fluid or drilling mud, down the inside of the drillstring, and out through nozzles in the drill bit. The fluid then travels up the annular space between the drillstring and borehole wall carrying with it cuttings particles in suspension. Once the fluid is returned to the drilling rig the cuttings particles are separated from the fluid by shale shakers. A shale shaker is a vibrating screen used to clean the drilling fluid of cuttings before it is pumped back down the drillstring.

The process of removing cuttings from the wellbore is known as hole cleaning. Hole cleaning efficiency is dependant on multiple factors. The parameters that effect hole cleaning efficiency are often segmented into cuttings parameters, fluid parameters and operational parameters(Sayindla (2018)). Cuttings parameters include cutting shape, cutting density, cutting size and cuttings concentration. Generally speaking, it is difficult to affect cuttings parameters as these are largely dependant on the formation that is being drilled. Fluid parameters are easier to influence. These include fluid rheology, density and flow rate. Operational parameters are parameters such as drillstring eccentricity, drillstring rotation speed, well inclination, annuli size and rate of penetration. The experiments conducted in this thesis was focused on the hole cleaning effects of fluid parameters and operational parameters.

Insufficient cuttings transport is one of the primary contributors to increased torque and drag(Mingquin Duan (2009)), i.e increased downhole friction. Consequences of increased torque and drag includes increased power consumption which in turn means higher operational costs. Even worse, it may result in the drillstring becoming stuck and halting

the drilling operation. Delays in drilling operations have huge economical consequences due to lost time and extremely expensive rig rates. According to IHSMarkit (2019) the average rate for semi-submersible offshore drilling rigs over the last couple of years have been between $130 000 and $300 000 per day. Good hole cleaning therefore has a huge impact on the cost constructing a well.

Most modern wells are deviated, i.e not vertical. In fact, many wells have a horizontal section. The economical gain of drilling deviated wells is unquestionable. A horizontal well is able to penetrate and drain far larger sections of a hydrocarbon reservoir, and thereby vastly increase the productivity of each well. The drawback of deviated wells is that it complicates hole cleaning. Most modern wells have both vertical, slanted and horizontal sections. The fluid properties required for good hole cleaning differs depending on the inclination of the well path. This means that it is impossible to have an ideal drilling fluid configuration throughout the well. In slanted and horizontal sections cuttings will accumulate on the low side of the borehole due to the reduced vertical component of the fluid flow. As a result, a bed of cuttings will establish. The drillstring slamming that is discussed throughout this thesis aims to reduce the height of such cuttings beds, and thereby reduce torque and drag.

The results presented in this thesis were obtained by flow loop experiments. Flow loops are used in many different fields of research. In general, a flow loop is any type of loop rig used to study behaviour involving flowing fluids, such as phase interactions during multi-phase flow. In relation to cuttings transport, flow loops are designed to emulate a wellbore. Flow loops provide a relatively cost-effective way of studying how cuttings transport is affected by cuttings parameters, fluid parameters and operational parameters. Insights gained from flow loop research aids in improving the design of future wells and drilling operations.

Chapter 2

Basic Theory

The entirety of this chapter is taken from Sandahl (2019). Sandahl (2019) documents the project work conducted during the fall of 2019. The project work consisted of planning and facilitating the present thesis. As such, the theory necessary to understand the experiments and results in this thesis are the same as for the project work.

2.1 Rheology

Rheology is an important factor in hole cleaning regardless of well inclination. This section will aim to summarize the basic terms and knowledge needed to appreciate the drilling fluid selection.

2.1.1 Shear Stress

Shear stress is the stress co-planar with a material's cross section defined as the force per unit area required to sustain a constant rate of fluid movement (Yunus A. Cengel (2010)). With respect to hole cleaning, shear stress describes the force transmitted from the fluid onto a cuttings particle. In figure 2.1, shear stress is the stress acting on the lower plate. The lower plate is stationary, while the upper plate is moving at a constant speed. The movement of the upper plate sets the fluid between the plates in motion which in turn transmits a stress on the lower plate.

2.1.2 Shear Rate

Shear rate is the rate of change of velocity at which one layer of fluid passes over an adjacent layer (Sandahl and Sørgård (2019)). In figure 2.1 the shear rate is defined by the flow velocity profile between the plates. This velocity profile occurs due to no-slip. No-slip means that the fluid in contact with the upper plate will move with the same velocity as the upper plate, v. Fluid in contact with the lower plate is stationary. Mathematically shear rate is expressed:

$$\dot{\gamma} = \frac{v}{h} \tag{2.1}$$

where v is velocity and h is the distance between the plates in figure 2.1.

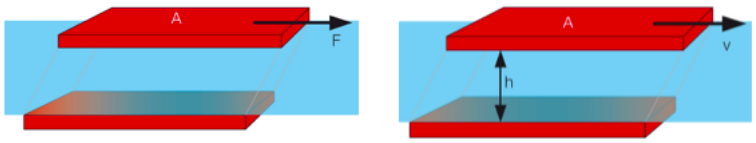

Figure 2.1: Two-Plate Model illustrating shear stress & shear rate. (Sandahl and Sørgård (2019))

2.1.3 Yield Stress

The yield stress(or yield point) is the shear stress needed to make a fluid flow. It is found by extrapolating a flow curve(plot of shear stress vs. shear rate) to zero shear rate.

2.1.4 Viscosity

Viscosity is a measure of a fluids internal resistance to flow. In the context of hole cleaning, viscosity is arguably the most important parameter. Viscosity is crucial as it is the property that enables the transferal of stress through a fluid as illustrated by by Newton's law of viscosity:

$$\tau = \dot{\gamma}\eta \tag{2.2}$$

where τ is shear stress, $\dot{\gamma}$ is shear rate and η is dynamic viscosity.

As the name suggests; Newtons law of viscosity applies to Newtionian fluids. For Newtonian fluids the viscosity is independent of shear rate, and has no yield point. A Newtonian fluid will therefore start to flow under any amount of shear stress. Also, the shear stress is directly proportional to shear rate.

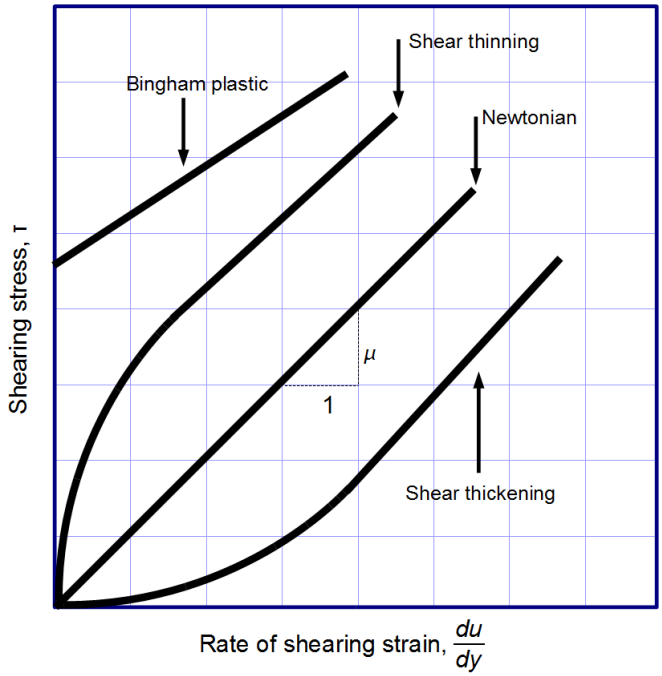

Figure 2.2: Schematic illustrating flow curves for different types of viscosity regimes. (wikipedia/viscosity (2019))

However, most drilling fluids are non-Newtonian. Fluids containing clay additives will typically exhibit thixotropic behaviour. **Thixotropy** describes the time dependence of a fluid with respect to viscosity. This is caused by buildup and breakdown of particle structures. These structures build up when the fluid is at rest, and breaks down when the fluid is sheared. Hence, a thixotropic fluid is shear thinning. This property allows the drilling fluid to flow easily when the mud pumps are running, and thicken to keep cuttings in suspension when circulation stops. A **Bingham plastic** fluid, as seen in figure 2.2, is a special type of fluid that act as a plastic until it is exposed to a sufficient amount of stress. Once this stress threshold(yield point) is reached, the viscosity is constant.

2.1.5 Viscoelasticity

Viscoelatic fluids are fluids that exhibit both viscous and elastic behaviour when deformed. That is, viscoelastic fluids exhibits both solid and liquid like behaviour. A characteristic of viscoelastic drilling fluids, in fact of all elastic materials, is the ability to exert a force on itself. Much like a rubber band, it will resist deformation and try to ”pull” itself together. Similar to the benefits of thixotropic fluids, viscoelasticity enables the drilling fluid to flow, but once the stress acting on the fluid is reduced it will regain strength which will help suspend cuttings particles.

2.2 Hole cleaning

Sufficient hole cleaning is a necessity for any well, and has been a popular topic of research for many years. In this section some of the basic physics and transport mechanisms of hole cleaning in different segments of a well will be discussed. To simplify, the well will be segmented in three parts: horizontal(90°-65°), tangential(65°-30°) and vertical(0°-30°). The reasoning behind this segmentation is that the flow regime, and thereby the cuttings transport, changes with inclination.

2.2.1 Vertical Hole Cleaning

In the vertical section cuttings transport efficiency is determined by the ratio of forces acting upwards versus forces pulling the cuttings downwards in the well. In other words, it is a battle between gravity pulling down and shear forces acting on the cuttings via the fluid flow pushing up. The simplest way of calculating the slip velocity, i.e the velocity of a particle slipping/sinking through a fluid, is to consider a single perfectly spherical particle slipping through a Newtonian fluid.

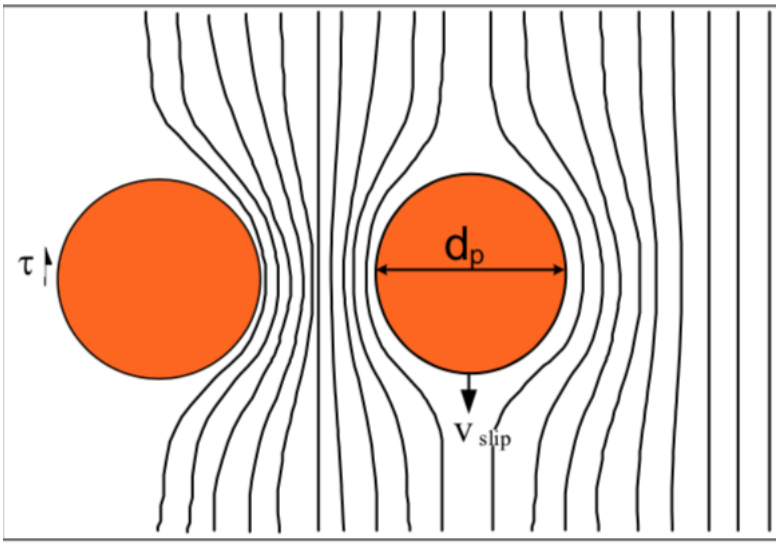

Figure 2.3: Two perfect spheres slipping through laminar flow. (Bjørn A. Brechan (2017))

As mentioned, there are only two forces involved in this scenario, gravity and shear force. The particle settles at a constant velocity when these forces are equal:

$$(\rho_{particle} - \rho_{mud})V_{sphere}g = \tau A_{sphere} \tag{2.3}$$

$$V_{sphere} = \frac{4}{3}\pi r^3 \tag{2.4}$$

$$A_{sphere} = 4\pi r^2 = \pi d_p^2 \tag{2.5}$$

where ρ is density, V_{sphere} is the volume of a sphere, g is acceleration due to gravity, τ is shear stress, A_{sphere} is the area of a sphere, r is radius and d_p is particle diameter.
The shear stress of a Newtonian fluid is defined as:

$$\tau = \mu \frac{dv_x}{dr} \tag{2.6}$$

where v_x is the velocity of the fluid flow in the axial direction through the borehole. The flow velocity is dependent on the distance from the borehole wall due to the no-slip condition as illustrated in figure 2.4.

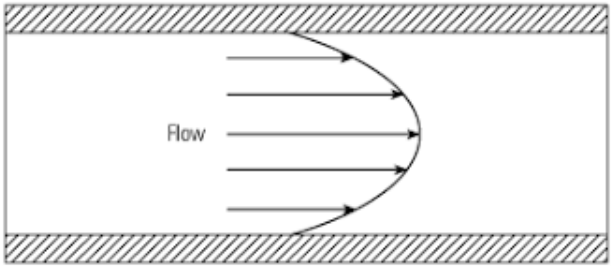

Figure 2.4: Flow velocity profile for pipe flow and no-slip along the walls. (igem.org/FluidDynamics (2018))

Assuming a small particle, such that the velocity with respect to the fluid flow velocity profile in the borehole can be assumed constant in the vicinity of the particle. The axial velocity of the fluid will only depend on the difference of path caused by the particle. Hence, the fluid velocity relative to the moving sphere is proportional to the distance through the center of the particle versus the distance along the periphery of the particle.

$$\frac{v_x}{v_{slip}} = \frac{v_{periphery}}{v_{center}} = \frac{\pi r}{2r} = \frac{\pi}{2} \implies v_x = \frac{\pi}{2} v_{slip} \tag{2.7}$$

The relative velocity change across the half sphere can then be expressed as:

$$\frac{dv_x}{dr} = \frac{\frac{\pi}{2} v_{slip}}{r} = \frac{\pi}{d_p} v_{slip} \tag{2.8}$$

Combining equations 2.3, 2.4, 2.5, 2.6 and 2.8:

$$(\rho_p - \rho_{mud}) \frac{\pi}{6} d_p^3 g = \mu \frac{\pi}{d_p} v_{slip} \pi d_p^2 \tag{2.9}$$

Solving for v_{slip}:

$$v_{slip} = \frac{(\rho_p - \rho_{mud}) d_p^2 g}{6\mu\pi} \tag{2.10}$$

Equation 2.10(Stokes law) is only valid for a single perfectly smooth sphere in a Newtonian fluid for very low Reynolds numbers along the surface of the particle($N_{Re} \leq 1$ (Bjørn A. Brechan (2017))). Also, it is only valid for particles with a radius of 1 mm or less (Bjørn A. Brechan (2017)). As such, it has no real value for hole cleaning other than providing some understanding of the forces and physics in play.
However, several correction functions exists that can be applied to account for higher particle concentrations. These aim to correct for the flow changes that occur when particles settle in close proximity to each other. As explained above, the fluid that flows along the periphery of a sphere is accelerated due to the increased path length. This causes the effective flow velocity to increase, and thus, also the shear rate and thereby the shear stress which ultimately implies slower settling velocity.

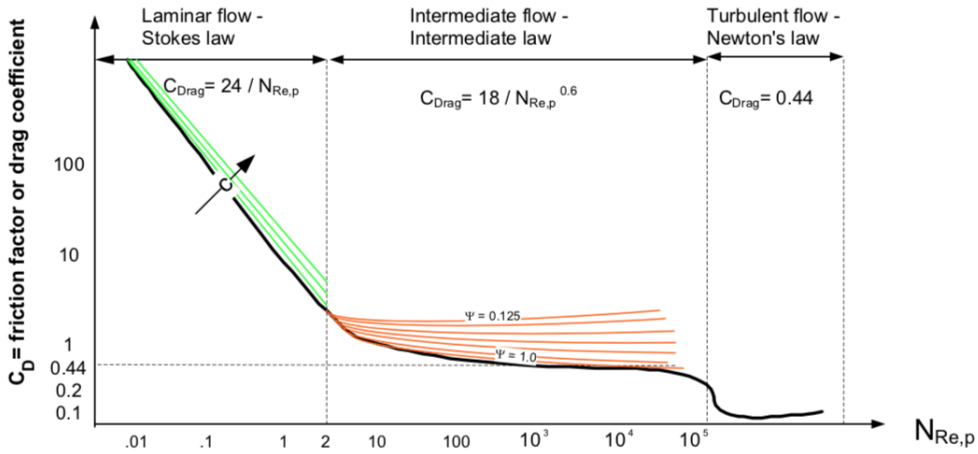

Figure 2.5: Drag coefficient of real particles as a function of Reynolds Number and flow regime in Newtonian fluids. (Bjørn A. Brechan (2017))

Although there exist correction functions that account for higher particle concentrations in Stokes law they do not account for different geometries and flow regimes. Cuttings are not perfect spheres. To account for different flow regimes a drag coefficient, C_{drag}, is introduced. The drag coefficient is derived empirically, and will change according to Reynolds number and flow regime as illustrated in figure 2.5. A drag force, F_{drag}, replacing the shear stress as a function of shear rate can be defined:

$$F_{drag} = C_{drag} \frac{\pi}{8} d_p^2 \rho_{mud} v_{slip}^2 \tag{2.11}$$

The force due to gravity, F_g:

$$F_g = \pi \frac{d_p^3}{6} (\rho_p - \rho_{mud}) g \tag{2.12}$$

Exploiting that the terminal settling velocity occurs when $F_g = F_{drag}$ the slip velocity is found:

$$v_{slip} = \sqrt{\frac{4(\rho_p - \rho_{mud})g}{3\rho_{mud}C_d}} \tag{2.13}$$

2.2.2 Horizontal Hole Cleaning

In contrast to the vertical section of a well, where cuttings are suspended in the drilling fluid, hole cleaning efficiency in the horizontal section of a well is a lot less affected by fluid rheology. This is due to the very limited vertical distance a cuttings particle has to travel before settling on the low side of the borehole. Furthermore, the fluid flow will be in the horizontal direction which results in a minimum lift force acting on the cuttings particle. The main transport mechanism in horizontal wells is therefore rolling and skipping, rather than suspension and lifting, as illustrated in figure 2.6. Once a particle has settled on the bottom of the borehole it has little chance of being resuspended in the fluid flow, and a cuttings bed will start to develop. Hole cleaning in horizontal wells is therefore a function of shear stress, fluid density, buoyancy, gravity and cohesive forces between the cuttings particles. Shear stress and density(momentum forces) are the easiest factors to influence.

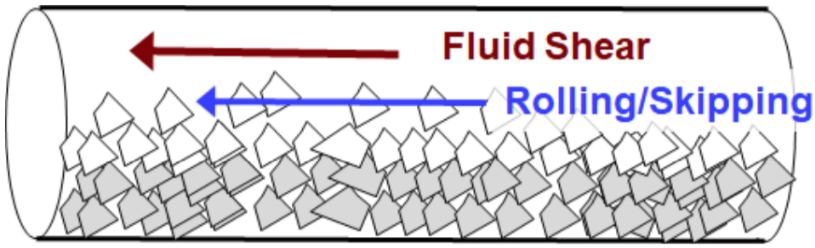

Figure 2.6: Rolling/skipping is the primary cuttings transport mechanism in a horizontal well

In a 90° wellbore, i.e a perfectly horizontal wellbore, a cuttings bed will quickly develop. The height of the cuttings bed is largely determined by the flow rate of the drilling fluid. The cuttings bed will continue to grow until it reaches an equilibrium. The equilibrium occurs because the cross sectional area of the wellbore is reduced due to cuttings bed buildup which leads to increased flow velocity. Higher flow velocity implies higher shear stress and momentum forces. However, achieving good hole cleaning in horizontal wells is not as simple as ramping up the flow rate, increasing the viscosity or increasing the density of the fluid. Increasing the flow velocity, fluid viscosity or density implies increasing the annular pressure drop. Consequently, the equivalent circulating density(ECD) is increased and may compromise borehole stability (Haugan (2019)). Furthermore, though a fluid with a higher viscosity results in a higher shear stress acting on the cuttings, Mingquin Duan (2009) found that low viscosity drilling fluids performed better with respect to sand bed removal. This suggests that momentum forces dominates with respect to hole cleaning in

highly deviated wellbores. Sifferman and Becker (1992) concludes that small increases in drilling fluid density reduces cuttings bed height significantly. This supports the claim that momentum forces are the primary driving force in highly deviated hole cleaning. This is also reflected in the drag force equation(eq. 2.11) where both density and velocity are key parameters.

As the inclination decreases the lift force becomes increasingly important for cuttings transport as illustrated in figure 2.7. The fluid flow will now have a vertical component that contributes to hole cleaning through lift. Also, the gravity contribution to the normal force will be reduced. Consequently, the particle-to-particle friction is reduced. Interestingly, this seems to have little impact on the hole cleaning effectiveness. Sayindla (2018) found only a slight improvement in hole cleaning effectiveness when comparing inclinations of 60° to 90°.

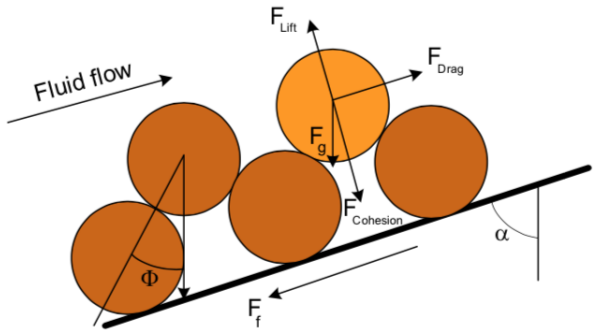

Figure 2.7: Schematic of forces involved in cuttings transport in a highly deviated well. Φ is angle of repose, α is inclination, F_{lift} is lift force, F_{drag} is drag force, F_g is gravity, $F_{cohesion}$ is cohesion force and F_f is friction force. (Bjørn A. Brechan (2017))

A proven method of reducing the cuttings bed height in highly deviated wells is drillstring rotation. When a cuttings bed is present the flow velocity near the bed will be significantly lower than the pumping rate due to no-slip. Consequently, the flow velocity in the upper part of the wellbore is higher. Additionally, this effect is exaggerated as the drillstring tends to lie on the low side of the wellbore. Ironically, this results in good hole cleaning potential in the part of the wellbore with the lowest cuttings concentration, and vice versa, as is evident from figure 2.8.

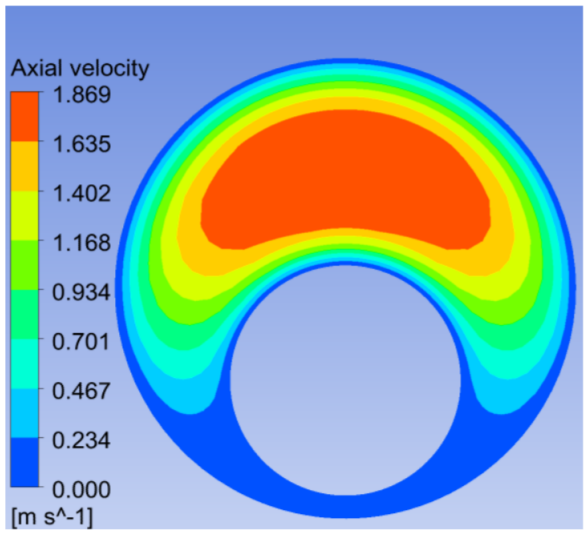

Figure 2.8: Map of fluid velocity in a wellbore with eccentric drillstring. Cutting in the higher flow velocity regions will travel further before settling in the cuttings bed. Cuttings transport is more effective if cuttings particles can be brought into high velocity regions of the wellbore. Pumping rate is 1 m/s. (Sayindla (2018))

By rotating the drillstring at a sufficent RPM cuttings are thrown into the high velocity region of the wellbore where they are more effectively transported up the annulus. When the drillstring is rotated shear forces are transmitted through the drilling fluid acting on the cuttings particles. This assists in disloging the cuttings from the cuttings bed. As a result the cuttings bed height is significantly reduced.

2.2.3 Tangential Hole Cleaning

Angle Φ in figure 2.7 is the angle of repose. The angle of repose is the angle where avalanches will naturally occur. As the cuttings bed builds up, particles will start to avalanche down the annulus and accumulate. Avalanching is characteristic of the tangential hole section. The transport mechanism for this section of the well is a mix of the mechanisms described for the horizontal and vertical sections. Depending on whether the inclination is closer to horizontal or vertical, the horizontal or vertical transport mechanisms will be more pronounced. This mixture of transport mechanisms makes specific rheology design problematic for the tangential section. There seems to be very little detailed research on the transport mechanisms in this section although it is firmly established that the sections where avalanches occur are some of the most challenging, if not the most challenging. Okrajni and Azar (1986) identifies 40°-45° as the most challenging inclination with respect to hole cleaning, underlining that the difficulties are caused by cuttings avalanching. Okrajni and Azar (1986) also comment on the potential need for further investigation of hole cleaning in the tangential section.

Chapter 3

Previous Work

The fall of 2019 was spent planning and conducting necessary research to facilitate the present thesis. The planning, literature review and research is documented in Sandahl and Sørgård (2019) and Sandahl (2019). However, since both of these works are so closely linked to this thesis their key considerations, findings and conclusions are summarized in this chapter.

3.1 Flow loop design improvements

Sandahl (2019) documents the preliminary testing, and suggested improvements, of the old flow loop setup used in Haugan (2019). The old flow loop setup is depicted in figure 3.1. During preliminary testing it became apparent that the cuttings injection system needed to be reworked.

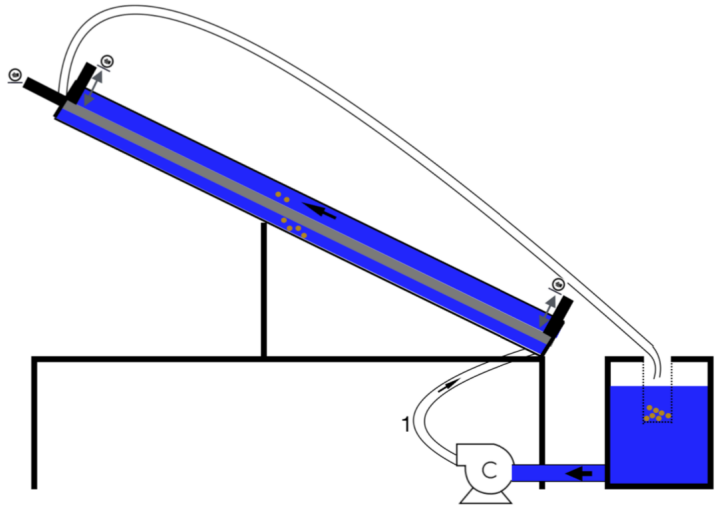

Figure 3.1: Flow loop schematic of the setup used in Haugan (2019).(Haugan (2019))

The loading procedure consisted of detaching the tube marked as 1 in figure 3.1 and manually pouring sand into the tube. The tube would then be reattached, and the pump would be turned on at maximum outlet pressure to inject the cuttings into the annular space. The main drawback to this procedure was that the sand would often get stuck and pack off to an unpredictable degree. Once the sand got unstuck it would jet into the annular space. The pump then had to be manually choked to avoid jetting the cuttings too far up the annular space. Sometimes it ended up in a pile by the inlet. Other times the sand would be evenly distributed. As a result of the unpredictability of the cuttings injection system it was impossible to achieve consistent initial conditions, and test results.

Two different cuttings injection system redesigns were considered:

- Installing a pump that could circulate slurry
- Installing a separate cuttings injection system, and a separation unit

Both designs focused on enabling continuous feeding of cuttings. Continuous feeding would make it possible to reach an equilibrium bed height, which would remove a lot of the human influence on the initial conditions and thereby improve repeatability. Continuous feeding of cuttings would also enable experiments on cuttings transport while drilling. Furthermore, if one wanted to a use computational fluid dynamics model(CFD) for comparison, it would require a uniform bed height as a starting point(Haugan (2019)). Achieving a more or less uniform bed height would be far easier with continuous cuttings feeding.

The separate cuttings injection system discussed in Sandahl (2019) would utilize a screwpump to feed sand into the flow loop. Such a screw pump would enable to operator to adjust the rate of cuttings injection, and thereby the cuttings concentration, in real-time. A drawback to this method is the increased complexity. Such a setup would require a tank to continuously feed cuttings into the screwpump. A separation unit would also be required.

Installing a pump capable of pumping slurry would be considerably easier to implement. However, this solution also required additional redesign. Since this design philosophy relies on circulating a slurry, two fluid reservoirs are required. One dirty reservoir containing the slurry, and a clean reservoir that enables tests on circulation without drilling, i.e circulation without sand particles. An agitator would also be required to keep sand concentrations evenly distributed throughout the dirty reservoir. Compared to the screwpump solution adjusting the sand concentration in the slurry is more tedious.

Ultimately the slurry pump solution was chosen due to its relative simplicity, and low redesign cost.

3.2 Fluid Design and Characterization

Sandahl and Sørgård (2019) documents several fluid characterization experiments conducted during the fall of 2019. The aim of Sandahl and Sørgård (2019) was to find suitable fluids to be used for the flow loop experiments in this thesis, as well as for Sørgård's thesis on surge and swab effects. The primary considerations with respect to fluid design was to achieve:

- Fluid transparency
- Realistic viscosity
- Realistic density

Transparency was prioritized to allow for visual observation of cuttings transport mechanisms during flow loop runs. Viscosity was emphasized as it is the primary fluid property that contributes to shear stress, and thus is one of the most important fluid properties that affects hole cleaning in medium deviation and vertical wells. Density also has a significant impact on hole cleaning as it is the primary contributor to both buoyancy and momentum forces. The density of a fluid will therefore largely influence hole cleaning in all sections of

a well. Another priority was to have as simple fluids as possible, i.e ideally no thixotropic, viscoelastic or plastic behaviour. It was also decided to only use one additive per fluid.
The bulk of the characterization work were conducted on an Anton Paar MCR 302 rheometer. The Anton Paar MCR 302 is capable of testing a fluid's shear stress dependency on shear rate and temperature, and thereby the fluid's viscosity at different temperatures and at different rates of shear. The Anton Paar MCR 302 is also capable of identifying, and quantifying, a fluid's thixotropic, plastic and viscoelastic properties.

After discussions with experienced staff at the Department of Geoscience and Petroleum at NTNU and SINTEF it was decided to test 2 glycerol based fluids, as well as 2 different mixtures of water and xanthan gum. The viscosity, density and mixing ratios can be found in table 3.1. It is important to note that the viscosity in table 3.1 is given at 28°C. The temperature in the lab where the flow loop is installed is roughly 18-22°C depending on the outside temperature. This implies that the viscosity likely was a little higher during the experiments discussed in chapter 5.

Table 3.1: Test Fluid Composition, η is given at 28°C and $\dot{\gamma}$ = 404 $1/s$. (Sandahl and Sørgård (2019))

Fluid Name	Additive	Water $[Wt-\%]$	Amount $[Wt-\%]$	ρ $[Kg/m^3]$	η $[cp]$
Xanthan Gum 1	Xanthan Gum	99.9	0.1	1000.5	7.06
Xanthan Gum 2	Xanthan Gum	99.8	0.2	1001	14.3
Glycerine 70	Glycerol	30	70	1140	10.3
Glycerine 80	Glycerol	20	80	1160	16.4

Xanthan gum

Xanthan gum was selected for testing due to its popularity in the industry and its potency as a viscosifier. Due its potency it is possible to achieve realistic viscosities even with very small amounts of xanthan gum added. This characteristic enabled the xanthan gum mixtures to retain some degree of transparency. A drawback to the minuscule quantities of xanthan gum added is that the densities of the xanthan gum mixtures were very close to water, as is evident from table 3.1. However, xanthan gum fluids are known to have a very flat velocity profile in annular flow (Sandahl and Sørgård (2019)). A flat velocity profile aids in the lifting and transport of cuttings particles, which to some degree remedies the low density.

Glycerol

Glycerol was chosen for testing due to its excellent viscosifying capabilities in high concentrations. In contrast to xanthan gum, the lack of potency is a positive attribute of glycerol as glycerol itself is perfectly transparent. Its lack of potency therefore enables the glycerol based fluids to achieve more realistic densities whilst retaining good viscosity and transparency. Glycerol is also a known Newtonian fluid.

3.2.1 Results

Figures 3.2, 3.3 and 3.4 illustrates the transparency of the glycerol 80 wt-% mixture as well as the two xanthan gum fluids. Both xanthan gum mixtures were somewhat opaque, although the 0.2 wt-% mixture were considerably worse with respect to transparency. Both of the glycerol mixtures looked identical and were as transparent as tap water.

Figure 3.2: Picture illustrating the transparency of the glycerol 80 wt-% mixture

Figure 3.3: Picture illustrating the transparency of the 0.1 wt-% xanthan gum mixture

Figure 3.4: Picture illustrating the transparency of the 0.2 wt-% xanthan gum mixture

Figures 3.5 and 3.6 depicts the flow curve plots generated by the Anton Paar MCR 302 when ramping up the shear rate from 1-1200 $1/s$ at a constant temperature of 28°C. As expected the glycerol mixture behaves perfectly Newtonian. In figure 3.6, the xanthan gum 0.1 wt-% mixture clearly displays shear thinning behaviour up to a shear rate of approximately 200 $1/s$. Shear thinning indicates either thixotropic or viscoelastic behaviour. At a shear rate of roughly 550 $1/s$ an apparent thickening occurs. At even higher rates of shear the curve starts to spike. Both of these phenomena are addressed in Sandahl and Sørgård (2019). However, since both effects occur at shear rates in excess of 500 $1/s$ it is not relevant for the flow loop employed in this thesis. In order to investigate the shear thinning behaviour that occurs at lower shear rates for the xanthan gum mixture a hysteresis loop test was conducted. The results are displayed in figure 3.7. Evidently, there is no sign of thixotropic behaviour in hysteresis loop test. Each run perfectly overlaps. This confirms that the xanthan gum mixtures displays inherent viscoelastic behaviour.

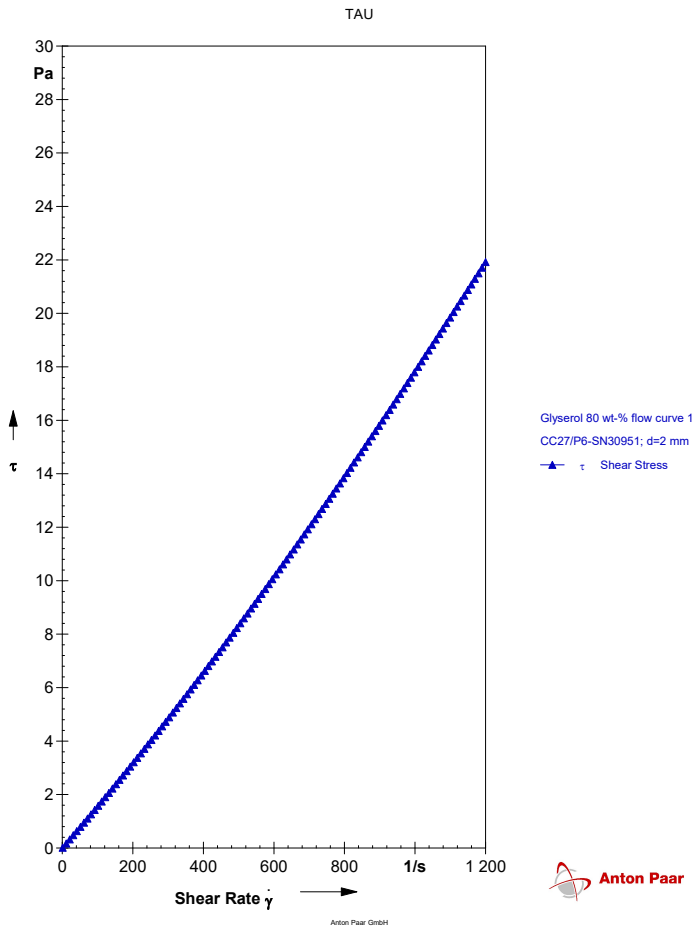

Figure 3.5: Flow curve for the 80 wt-% glycerol mixture generated by Anton Paar MCR 302. The temperature was held at a constant 28°C.

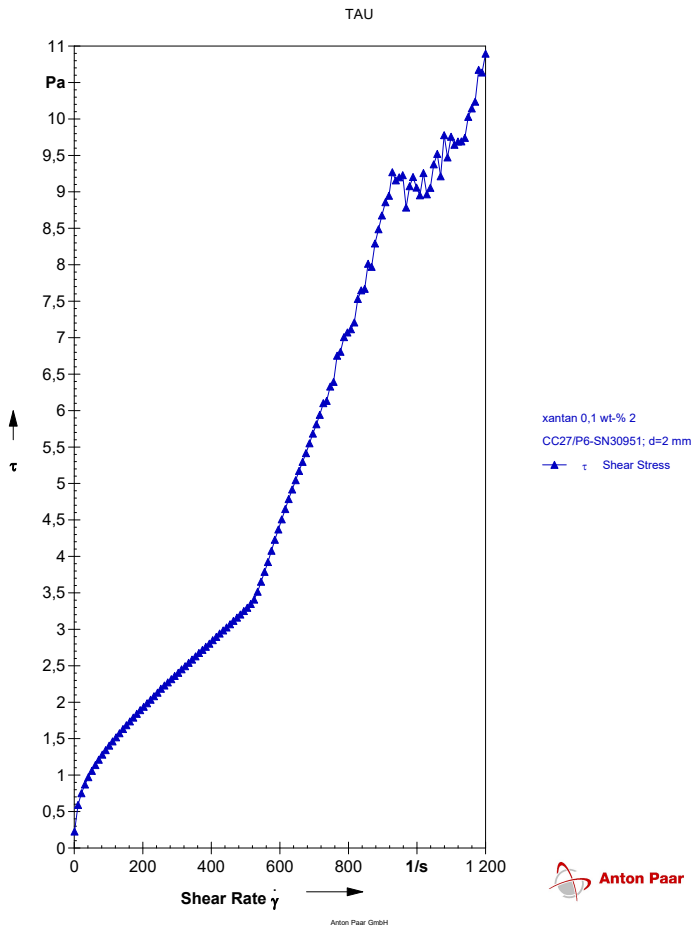

Figure 3.6: Flow curve for the 0.1 wt-% xanthan mixture generated by Anton Paar MCR 302. The temperature was held at a constant 28°C.

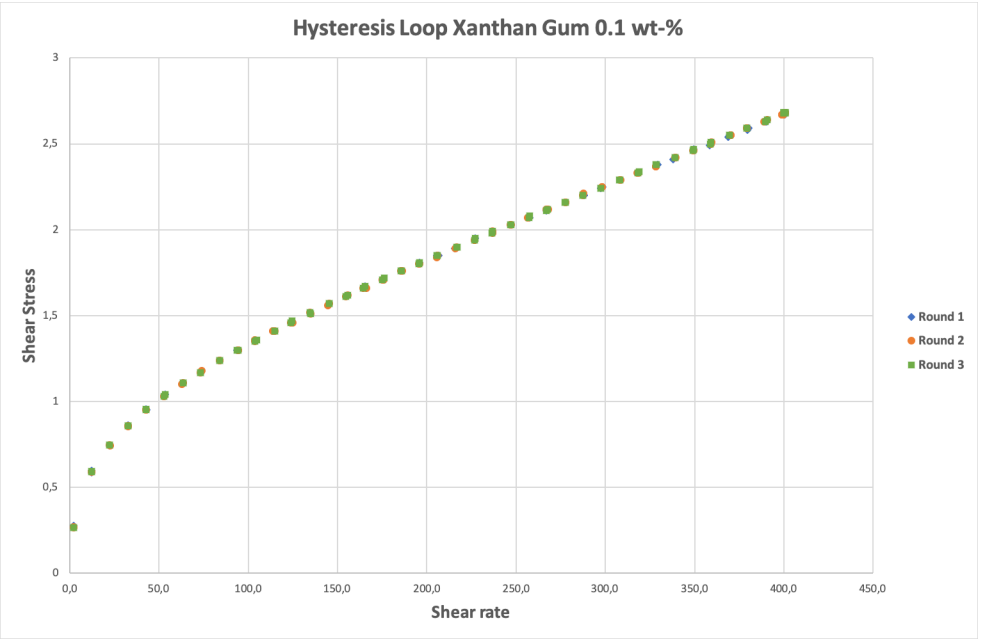

Figure 3.7: Hysteresis loop test for xanthan gum 0.1 wt-%

3.2.2 Conclusion

The xanthan gum mixtures were ruled out due to the complicating viscoelastic behaviour. Also, the glycerol mixtures displayed favorable transparency and density. It was concluded that the glycerol 80 wt-% glycerol mixture would be the fluid of choice going forward due to the inherent Newtonian behaviour, supreme transparency, as well as favorable viscosity and density compared to the glycerol 70 wt-% mixture.

Chapter 4

Experiment

4.1 COVID-19

Due to the coronavirus NTNU closed on March 12 2020. The campus shutdown included the closing of all labs. NTNU also put a hold on all equipment and supply orders. This hold affected most of the parts for the flow loop redesign as mentioned in section 3.1, as well as the glycerol order. The labs partly re-opened for critical personnel and students who needed access to labs to finish their theses on April 27 2020. However, due to the hold on orders much of the needed equipment was missing. Due to the normally short delivery times of glycerol, the order had not been placed before the hold was put in effect. The order for glycerol was therefore not sent until April 28. Unfortunately, due to the increase in hand sanitizer consumption as a result of the pandemic, the required volumes of glycerol was no longer available. Consequently, the planned glycerol based fluid had to be dropped.

As a result of the aforementioned delays, the flow loop was not operational until May 6. At this point, suited cuttings concentrations and experimental procedures needed to be established. In turn, experimentation did not commence until May 15. Due to the limited time available it was decided to drop roughly 80% of the planned experiments. The original experiment plan can be found in appendix A.1

4.2 Fluids

One of the most important improvements suggested in Sandahl (2019) was to conduct testing with more viscous fluids than water. Both Sandahl (2019) and Sandahl and Sørgård (2019) concluded that the 80 wt-% glycerol fluid was preferable. However, due to the complications discussed in section 4.1, the preferred glycerol fluid was not available for the tests conducted in relation to this thesis. It was therefore decided to conduct the experiments using the 0.2 wt-% xanthan gum fluid, due to its preferable viscosity versus the 0.1 wt-% xanthan gum fluid, although the higher xanthan gum concentration meant reduced

transparency and increased viscoelastic effects. Figure 4.1 depicts the flow curve for the xanthan gum fluid used in these experiments. Its properties are listed in table 4.1.

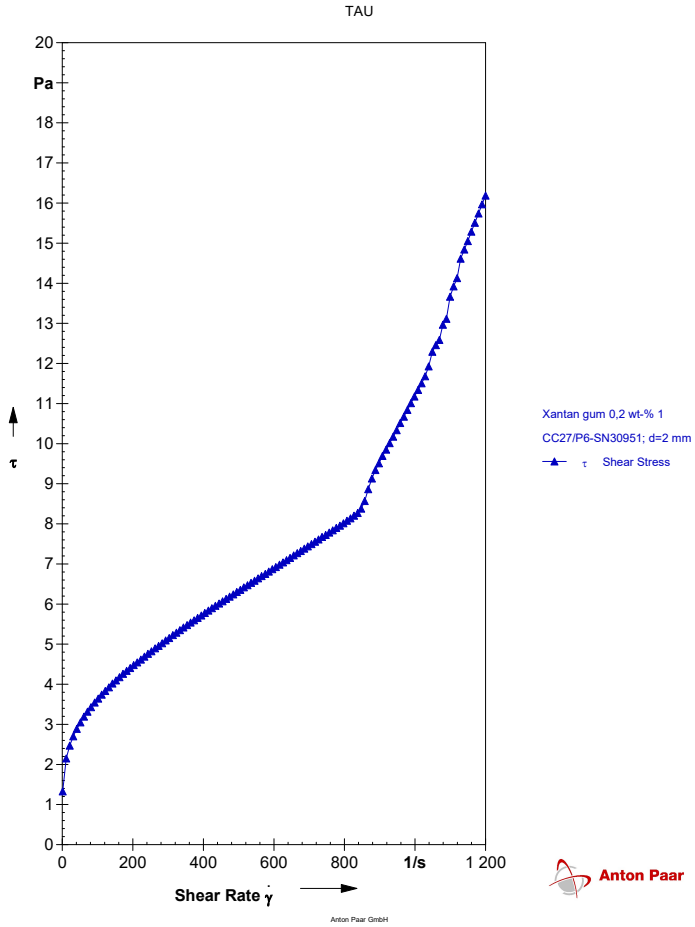

Figure 4.1: Flow curve generated by the Anton Paar MCR 302 rheometer for the 0.2 wt-% xanthan mixture used in the following experiments. The temperature was held at a constant 28°C.

Table 4.1: Properties of the xanthan gum fluid used for experimentation, η is given at 28°C and $\dot{\gamma}$ = 404 $1/s$. (Sandahl and Sørgård (2019))

Fluid Name	Additive	Water $[Wt-\%]$	Amount $[Wt-\%]$	ρ $[Kg/m^3]$	η $[cp]$
Xanthan Gum 2	Xanthan Gum	99.8	0.2	1001	14.3

4.3 Flow Loop Setup

The flow loop setup used in the experimental work described in this thesis is an evolution of Haugan (2019)'s setup. Much of the preliminary work leading up to the experiments conducted in this thesis was focused on finding areas of improvement in Haugan (2019)'s setup and procedures. Sandahl (2019) gives an in depth account of criticisms and plans for improvement on Haugan (2019), most of which have been implemented in the current setup. These design changes are summarized in section 3.1.

Figure 4.2 displays the flow loop setup used for the experimental work in this thesis. Its main component is the test tube marked as 8 in figure 4.2. It consists of a transparent 2 m long PMMA plastic tube with an inner diameter of 70 mm, and with a 38 mm stainless steel drillstring inside. The test tube inclination is adjustable and can be set to 90°, 60°, 45° and 30° by moving a strut bar. The low side of the test tube is covered in fine grained plastic particles to emulate the roughness of a borehole wall. This roughness is essential to allow for cuttings bed buildup. Figure 4.3 depicts a shard of the PMMA tube with plastic particles. There is a linear motor at either end of the test tube. These motors are marked as 7 and 9 in figure 4.2. The motors are used to adjust the eccentricity of the stainless steel drillstring. They are fully programmable and synchronizeable, and can therefore also be used to make the drillstring oscillate or change eccentricity periodically. Item 10 in figure 4.2 is the rotational motor used to rotate the stainless steel drillstring. The rotational motor has a maximum speed of 750 RPM.

The test tube is fed by one of two reservoirs. There is a "dirty" reservoir containing sand particles in suspension, and a "clean" reservoir only containing clean liquid. These are marked as 2 and 12 in figure 4.2, respectively. Each of the reservoirs holds up to 120 liters of liquid. There is a cement mixer installed in the dirty reservoir which is used to keep the sand particles in suspension and prevent sand accumulation in the lower parts of the reservoir. The cement mixer is capable of 1044 RPM, but was limited to 300 RPM due to excessive vibration with the current setup at higher RPMs. The clean reservoir has a strainer fitted to the reservoir inlet to prevent sand from entering the clean reservoir. The strainer has a mesh size of 0.8 mm. The sand particles used had a diameter of approximately 0.9-1.1 mm. To avoid contamination of the clean reservoir; all sand that was put into the system was pre-filtered with a 0.8 mesh size strainer. The pump marked as 4 in figure 4.2 is capable of delivering a flow rate of approximately 120-150 liters per minute(lpm) depending on the concentration of sand particles in the fluid flow and test tube. The fluid return line(11 in figure 4.2) is flexible and can be placed into either reservoir. It is therefore possible to run the loop with either clean or dirty fluid. This enables experiments on hole cleaning under both while drilling as well as while circulating conditions.

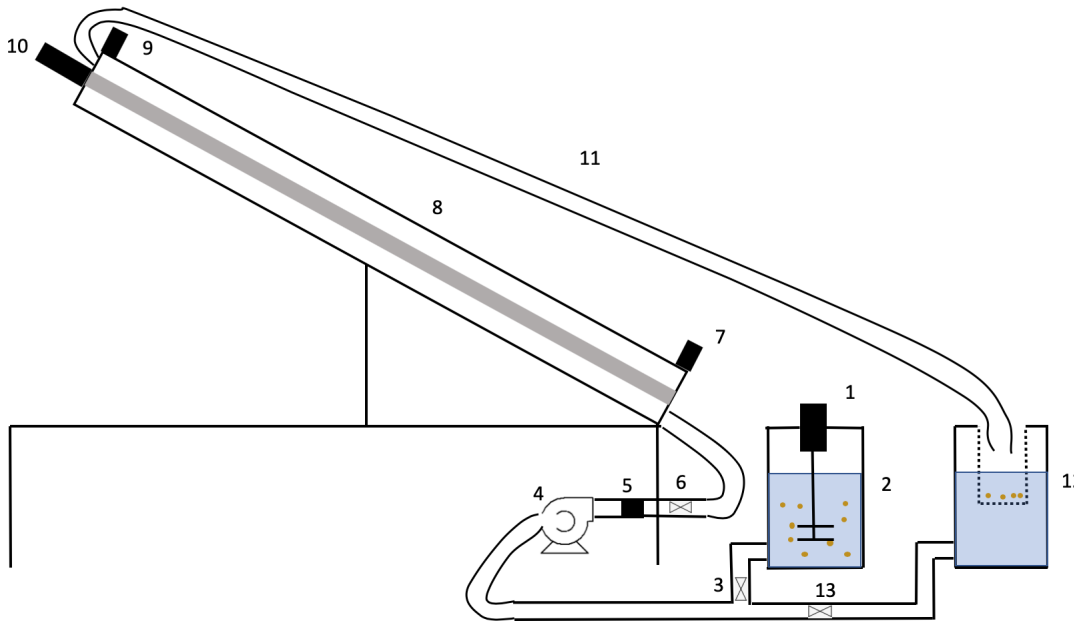

Figure 4.2: Schematic of the flow loop setup. 1) Agitator 2) Dirty reservoir 3) Dirty reservoir outlet valve 4) Pump 5) Flow rate sensor 6) Test tube inlet valve 7) Lower linear motor 8) Test tube 9) Upper linear motor 10) Rotational motor 11) Return line 12) Clean reservoir with a strainer at the inlet 13) Clean reservoir outlet valve

Figure 4.3: Picture of the fine grained plastic particles used to emulate borehole wall roughness that covers the lower side of the PMMA tube

4.4 Experimental Procedure

Before an experiment can begin it is paramount to be able to create easily repeatable starting conditions. As described in section 4.3, the flow loop setup employed in these experiments relies on circulation of a sand carrying fluid to introduce sand particles into the test tube (figure 4.2 part 8). To ensure repeatability of the experiments a set of loading parameters was established. These loading setting are detailed in subsection 4.4.1.

Loading

The experiment procedure starts with the flow loop drained, and with all valves closed. Both reservoirs are filled with 80 liters of liquid. 8 liters of filtered sand is added to the dirty reservoir(fig. 4.2 part 2), corresponding to a water/sand-ratio of 0.1. The drillstring is set in a negatively eccentric position, i.e the drillstring is resting at the bottom of the test tube(fig. 4.2 part 8). This is achieved by use of the linear motors(fig. 4.2 part 7 & 9). The rotational motor(fig. 4.2 part 10) is set to 150 RPM. The return line(fig. 4.2 part 11) is placed in the dirty reservoir. Before loading, the agitator(fig. 4.2 part 1) is run at 300 RPM for 2 minutes to ensure an even distribution of sand particles in the dirty reservoir. The pump (fig. 4.2 part 4) is then turned on at the frequency corresponding to the intended test settings. The dirty reservoir outlet valve(fig. 4.2 part 3) is opened. As the test tube inlet valve (fig. 4.2 part 6) is opened, timing begins. After the loading run is complete, the test tube inlet valve is closed to avoid backflow. The pump is shut off, and the dirty reservoir outlet valve is closed. The return line is placed into the strainer at the inlet of the clean reservoir(fig. 4.2 part 12).

Testing

The pump and motors are turned on at test specific settings, and the clean reservoir outlet valve(fig. 4.2 part 13) is opened. As the test tube inlet valve is opened test timing begins. After the test is completed the test tube inlet valve is closed to avoid backflow, and the pump is turned off. The amount of returned sand particles is measured by removing the strainer and weighing it.

Resetting

The strainer is placed back into the clean reservoir inlet, and the system is flushed clean by running the pump at maximum flow rate. Once the system is perfectly flushed, i.e there is no sand particles left in the test tube or return line, the test tube inlet valve is closed. The pump is turned off, and the clean reservoir outlet valve is closed. The dirty reservoir outlet valve is opened. The test tube inlet valve is then opened, allowing the fluid that is remaining in the test tube to flow back into the dirty reservoir. This allows the fluid level in both tanks to remain constant. The final step is to close all valves, and weigh the total amount of cuttings before pouring the contents of the strainer back into the dirty reservoir.

Resetting using the 0.2 wt-% xanthan gum fluid

When running tests using xanthan gum it proved difficult to perfectly clean the test tube. It was therefore decided to do timed cleaning runs, instead of cleaning the test tube perfectly. Other than that the resetting procedure was identical to the procedure detailed above. The cleaning run settings are listed below:

- Drillstring RPM: 375
- Drillstring eccentricity: Positively eccentric
- Pump frequency: 50 Hz, corresponding to $\approx$ 120 lpm
- Run time: 2 minutes

4.4.1 Loading Settings

- Drillstring RPM: 150
- Drillstring eccentricity: Negatively eccentric
- Pump frequency: 26 Hz, corresponding to $\approx$ 60 lpm
- Loading time: 5 minutes

4.4.2 Experimental settings

As explained in section 4.1 the volume of experiments had to be reduced compared to the original plan. It was decided to focus on 60° inclination relative to vertical. 60° inclination was emphasised as it is the inclination where avalanching starts to occur. It was also noticed during preliminary testing that steeper angles were more influenced by vertical hole cleaning mechanisms than expected. As such, steeper angles were considered less suited for testing of the potential of drillstring slamming. Furthermore, during preliminary testing to determine the experiment procedures using water it was observed that the cuttings bed slid down and caused a pack-off when the pump was turned of during testing at 45°. Consequently much of the flow loop setup had to be disassembled and cleaned to get the flow loop working again. Additionally, these problems would make it very time consuming to obtain reliable results and thereby jeopardize the entire thesis work.

Four experiments were conducted for each fluid. Each experiment was repeated three times to evaluate the repeatability of the experiments, and thereby the effectiveness of the cuttings injection design. The experiments were as follows:

- **Circulation**: Negatively eccentric drillstring placement, no eccentricity variation(drillstring slamming), 60° inclination, no drillstring rotation, clean fluid circulated at 60 lpm for 4 minutes
- **Circulation and drillstring rotation**: Negatively eccentric drillstring placement, no eccentricity variation(drillstring slamming), 60° inclination, 150 RPM drillstring rotation, clean fluid circulated at 60 lpm for 4 minutes
- **Circulation and drillstring slamming**: Drillstring slamming at 5 second intervals, 60° inclination, no drillstring rotation, clean fluid circulated at 60 lpm for 4 minutes
- **Circulation, drillstring rotation and slamming**: Drillstring slamming at 5 second intervals, 60° inclination, 150 RPM drillstring rotation, clean fluid circulated at 60 lpm for 4 minutes

Table 4.2: Motor settings used to achieve the lateral drillstring movement(slamming effect). v is velocity, a is acceleration, dec is deceleration, position is relative to positively eccentric drillstring

v m/s	a [m/s^2]	dec [m/s^2]	Lower pos [mm]	Upper pos [mm]
10	2	2	-18	0

Test Parameter Decisions

Since the tests were conducted at 60° inclination it was decided run all the tests with a negatively eccentric drillstring as this is most likely eccentricity when drilling at this inclination. It was also decided to rotate the drillstring at 150 RPM in the tests incorporating drillstring rotation. This may seem excessive. However, it was done to ensure that the

results would yield clear indications of the impact of drillstring rotation compared to the tests without rotation. Figure 4.4 illustrates the hole cleaning effects of drillstring rotation at different RPMs. It indicates that there is a sudden increase in hole cleaning efficiency at approximately 120 RPM. Rotating at 150 RPM ensured that the test results took advantage of this sudden improvement in hole cleaning performance.

The slams occurred at 5 second intervals. The 5 second intervals were chosen to reflect the time delay that would occur due to the elasticity of the drillstring. In reality, drillstring slamming would be induced by a jerking motion in the drawworks. It would therefore take some time for the motion instigated at the drawworks to propagate down to the slanted section of a well.

Both the 4 minute experiment run time, and the 60 lpm flow rate was chosen because it was found that a higher flow rate or a longer run time would result in too much sand being returned. It would therefore be difficult to differentiate the effects of the different parameters.

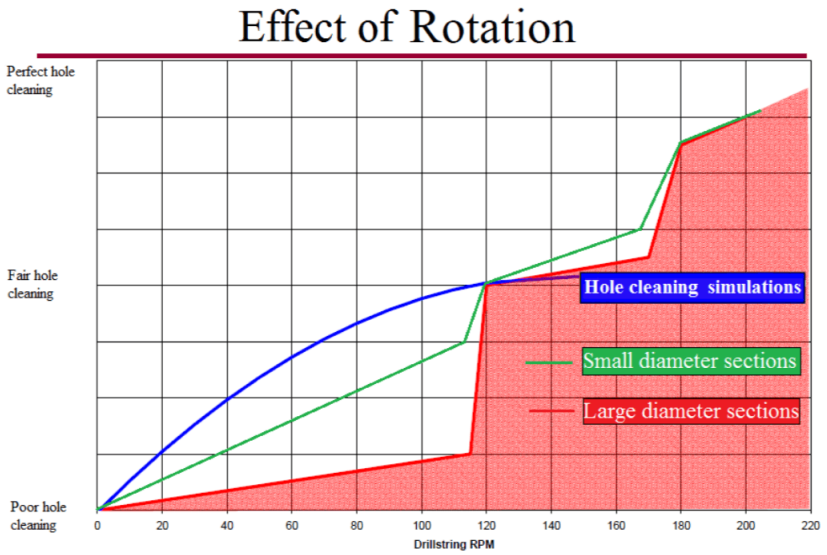

Figure 4.4: Plot illustration the hole cleaning effect of drillstring rotation vs. RPM (Bjørn A. Brechan (2017))

Chapter 5

Results and discussion

5.1 Experiments utilizing water at 60° inclination

During testing it was noticed that the linear motors used to adjust drillstring eccentricity occasionally fail when put under stress. Once one, or both, of the motors failed they would start to retract slowly, and thereby change the eccentricity of the drillstring. These failures occured both during loading of cuttings and testing. As these failures affected the eccentricity of the drillstring they also affected cuttings bed buildup and hole cleaning results. As a result several tests had to be discarded and redone. The most critical implication of these failures where that they severely affected the tests involving drillstring slamming. As the failures were triggered by stress, the throw of each drillstring slam had to be severely reduced to avoid failures when the drillstring impacted the cuttings bed.

Figure 5.1 depicts the bed height during the loading procedure using tap water. The bed height is clearly very high. However, this amount of cuttings were found to be necessary to achieve a reproducible bed height, i.e achieving an equilibrium bed height throughout the test tube for the given loading settings. Note that the bed height is significantly reduced when the drillstring is raised to either a concentric or positively eccentric position.

Figure 5.1: Picture of the equilibrium bed height during loading at 60° with a negetively eccentric drillstring rotating at 150 RPM and circulating water at 60 lpm.

Circulation

The circulation tests were conducted to establish a baseline for the following tests utilizing drillstring rotation and drillstring slamming. Table 5.1 contains the results of the circulation baseline tests. It is apparent that the loading of cuttings was fairly consistent throughout these experiments. It is also worth noting that there is a correlation between the initial amount of cuttings and the amount of cuttings successfully cleaned after each run. This is expected, as the effective flow rate in the vicinity of the cuttings bed increases as a function of cuttings bed height and thereby also increases hole cleaning efficiency. Figure 5.2 depicts the cuttings transport during these tests. It clearly shows how the cuttings rolls upwards and moves like a sand dune. By comparing figure 5.2 to figure 5.1 it is apparent that roatating the drillstring aids in keeping the bed height uniform.

Table 5.1: Hole cleaning results, circulating water at 60 lpm with at negatively eccentric drillstring for 4 minutes. $W_{cuttings_{test}}$ is the weight of cuttings removed after each test run. $W_{cuttings_i}$ is the initial weight of the cuttings in the test tube at the start of each run. Max $\Delta W_{cuttings_i}$ is the maximum difference in the initial amount of cuttings for the test.

Run	$W_{cuttings_{test}}$[kg]	$W_{cuttings_i}$[kg]	$Max\Delta W_{cuttings_i}$[kg]	Effectiveness[%]
1	3.13	4.68	0.12	67
2	2.87	4.56	0.12	63
3	2.90	4.57	0.12	63

Figure 5.2: Picture of the upper part of the test tube during a circulation only test run illustrating how the cuttings bed moves in the absence of drillstring rotation

Circulation and Drillstring Rotation

The tests involving drillstring rotation were conducted to allow for comparison of rotation, slamming and rotation and slamming combined. Table 5.2 contains the results of these tests. Surprisingly, there does not seem to be much improvement in hole cleaning by rotating the drillstring when circulating water. If anything, it seems to have a slight negative effect. By comparing table 5.1 and table 5.2 it is apparent that the initial amount of cuttings were a little higher during the circulation only runs. As such, no clear conclusion can be drawn. A possible explanation to the equal or reduced effectiveness is that the drillstring is more or less buried in the bed in the negatively eccentric position. Since the drillstring is submerged in the bed it will largely agitate the lower layers of the bed where the local flow velocity is extremely low or stagnant. It was observed that the lower layers of the bed slid downwards when rotating. This may equalize, or even outweigh, the positive effects of agitating the upper layers of the bed where the local flow velocity is considerably higher. Also, due to the low viscosity of water the cuttings that do enter the fluid flow quickly resettle which largely negates the positive effects of drillstring rotation.

Table 5.2: Hole cleaning results, circulating water at 60 lpm with a negatively eccentric drillstring and drillstring rotation of 150 RPM for 4 minutes. $W_{cuttings_{test}}$ is the weight of cuttings removed after each test run. $W_{cuttings_i}$ is the initial weight of the cuttings in the test tube at the start of each run. Max $\Delta W_{cuttings_i}$ is the maximum difference in the initial amount of cuttings for the test.

Run	$W_{cuttings_{test}}$[kg]	$W_{cuttings_i}$[kg]	$Max\Delta W_{cuttings_i}[kg]$	Effectiveness[%]
1	2.52	4.12	0.27	61
2	2.31	3.99	0.27	58
3	2.66	4.26	0.27	62

Table 5.3 displays the hole cleaning results for drillstring slamming without rotation when circulating water at 60 lpm. As described in the beginning of section 5.1 the throw of each slam had to be reduced from the initial 18 mm to 8 mm to avoid failures on the two linear motors used to adjust eccentricity. It is evident from table 5.3 that the hole cleaning during these runs were considerably better compared to table 5.1 and 5.2. During testing, however, it was observed that the increased hole cleaning effectiveness seemingly resulted from the periodically positively eccentric drillstring, rather than increased cuttings suspension due to the actual slams. When the drillstring is in the top of the test tube(positively eccentric drillstring) the flow velocity is increased in the low side of the test tube. The high flow velocity zone is therefore forced closer to the cuttings bed, which increases the cuttings transport rate and lowers the equilibrium bed height. Similar observations were made in Haugan (2019). Additionally, it was observed that every time the drillstring rested on the cuttings bed it arrested the cuttings transport by pinching the bed between the drillstring and the test tube wall. The observations made during these runs indicate that drillstring eccentricity is far more important than slamming when circulating water. Due to the low viscosity of water it is poorly suited to carry cuttings in suspension. The positive effect of each slam is therefore miniscule. Although it was observed that the upper layer of the cuttings bed is thrown up and into the fluid flow at each impact the cuttings quickly resettle. Figure 5.3 depicts the moment the drillstring slams into the cuttings bed.

Table 5.3: Hole cleaning results, circulating water at 60 lpm and slamming the drillstring at 5 second intervals for 4 minutes. $W_{cuttings_{test}}$ is the weight of cuttings removed after each test run. $W_{cuttings_i}$ is the initial weight of the cuttings in the test tube at the start of each run. Max $\Delta W_{cuttings_i}$ is the maximum difference in the initial amount of cuttings for the test.

Run	$W_{cuttings_{test}}$[kg]	$W_{cuttings_i}$[kg]	$Max\Delta W_{cuttings_i}$[kg]	Effectiveness[%]
1	3.30	4.19	0.38	79
2	2.79	3.84	0.38	73
3	3.18	4.22	0.38	75

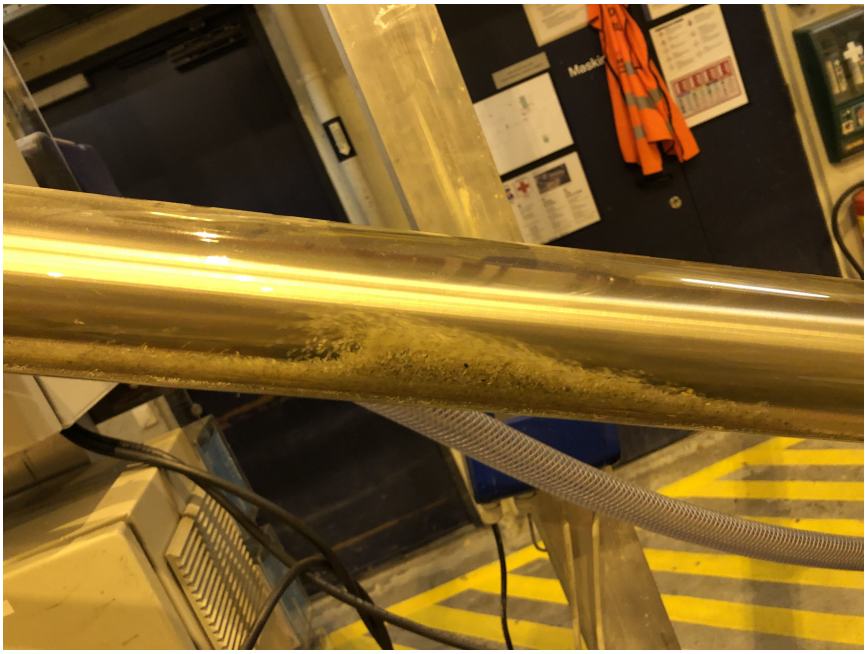

Figure 5.3: Picture of the moment where drillstring slams into the cuttings bed. The top layer of the cuttings bed is visibly lifted as a result of the impact and the displacement of water.

Circulation, Drillstring Rotation and drillstring Slamming

The results of the tests involving the combination of drillstring rotation and drillstring slamming indicates that combining rotation and slamming is less effective than slamming alone. Again, the likely explanation is the low viscosity of water as well as the aforementioned agitation of the lower layers of the cuttings bed caused by drillstring rotation and negative drillstring eccentricity. Also, as discussed above, the increased hole cleaning effect compared to table 5.1 and table 5.2 seemed to be caused by the eccentricity changes rather than the actual slam.

Table 5.4: Hole cleaning results, circulating water at 60 lpm with drillstring rotation of 150 RPM and slamming the drillstring at 5 second intervals for 4 minutes. $W_{cuttings_{test}}$ is the weight of cuttings removed after each test run. $W_{cuttings_i}$ is the initial weight of the cuttings in the test tube at the start of each run. Max $\Delta W_{cuttings_i}$ is the maximum difference in the initial amount of cuttings for the test.

Run	$W_{cuttings_{test}}$[kg]	$W_{cuttings_i}$[kg]	$Max\Delta W_{cuttings_i}$[kg]	Effectiveness[%]
1	2.56	3.92	0.34	65
2	2.68	4.10	0.34	66
3	2.83	4.26	0.34	66

5.2 Experiments utilizing water with 0.2 wt-% xanthan gum at 60° inclination

All the results discussed in this section were obtained using the 0.2 wt-% xanthan gum fluid detailed in section 4.2. Once experimentation commenced the effects of the fluid change became immediately apparent. Visually it was observed that a significant amount of sand particles were carried in suspension during the loading procedure as illustrated in figure 5.4. The equilibrium bed height was also significantly reduced compared to the loading runs using water. This reduction of the equilibrium bed height is likely caused by a combination of the flatter velocity profile of xanthan gum discussed in chapter 3.2, and the improved hole cleaning effect of drillstring rotation due to the increased viscosity. The effects of viscoelasticity on cuttings bed consolidation discussed in Sayindla (2018) was also noticed. Due to cuttings bed consolidation it proved difficult to clean the test tube perfectly after each run. These difficulties made the cleaning procedure detailed in section 4.4 necessary.

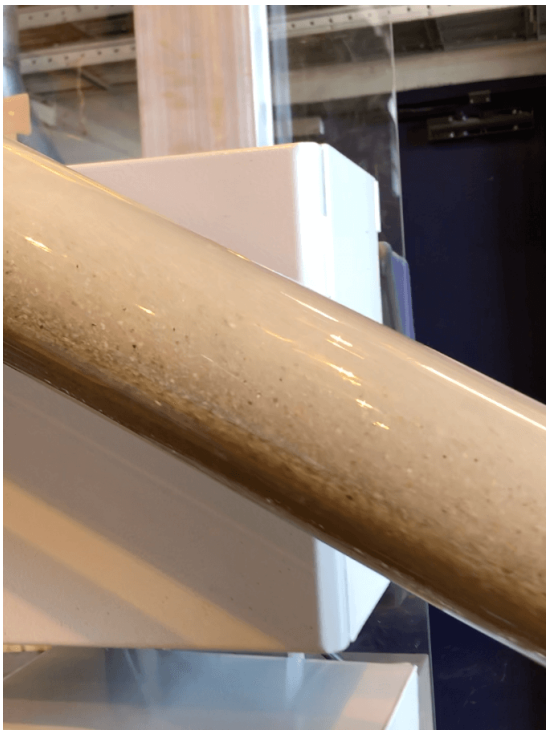

Figure 5.4: Picture illustrating sand particles being carried in suspension during the loading procedure using the 0.2 wt-% xanthan gum fluid.

Circulation

Table 5.5 contains the results of the test runs with fluid circulation alone. Surprisingly there was a huge discrepancy in the initial amount of sand particles in the test tube between run 1 and 2, and run 3. No good explanation for these discrepancies were found. However, by comparing table 5.5 to tables 5.6, 5.7 and 5.8 the amount of sand particles in run 3 seems to be more in line with the other tests.
The low cleaning effectiveness is explained by a combination of increased cuttings bed consolodation due to viscoelasticity, and the low equilibrium bed height during the xanthan gum tests compared to the water tests. There is simply less cuttings to clean during circulation runs. The difference can be observed by comparing figure 5.5 to figure 5.1. Also, due to the increased consolidation fluid circulation alone seemed to have a reduced effect. The 60 lpm flow rate was not high enough to dislodge significant amounts of sand particles from the cuttings bed.

Table 5.5: Hole cleaning results, circulating water with 0.2 wt-% xanthan gum at 60 lpm with a negatively eccentric drillstring for 4 minutes. $W_{cuttings_{test}}$ is the weight of cuttings removed after each test run. $W_{cuttings_i}$ is the initial weight of the cuttings in the test tube at the start of each run. Max $\Delta W_{cuttings_i}$ is the maximum difference in the initial amount of cuttings for the test.

Run	$W_{cuttings_{test}}$[kg]	$W_{cuttings_i}$[kg]	$Max\Delta W_{cuttings_i}$[kg]	Effectiveness[%]
1	0.40	2.35	0.80	17
2	0.32	2.26	0.80	14
3	0.16	1.55	0.80	11

Figure 5.5: Picture illustrating the bed height after a loading run using the 0.2 wt-% xanthan gum fluid

Circulation and Drillstring Rotation

Table 5.6 contains the hole cleaning results for the test runs with drillstring rotation in addition to fluid circulation. As expected, the increased viscosity of the xanthan gum fluid enhances the effect of drillstring rotation on hole cleaning. Comparing table 5.6 to table 5.5 we observe an increase of 42-56 % in hole cleaning efficiency. It is also worth noting that this increase was not observed in the tests using water.

Table 5.6: Hole cleaning results, circulating water with 0.2 wt-% xanthan gum at 60 lpm with a negatively eccentric drillstring and drillstring rotation of 150 RPM for 4 minutes. $W_{cuttings_{test}}$ is the weight of cuttings removed after each test run. $W_{cuttings_i}$ is the initial weight of the cuttings in the test tube at the start of each run. Max $\Delta W_{cuttings_i}$ is the maximum difference in the initial amount of cuttings for the test.

Run	$W_{cuttings_{test}}$[kg]	$W_{cuttings_i}$[kg]	$Max\Delta W_{cuttings_i}[kg]$	Effectiveness[%]
1	0.95	1.52	0.24	62
2	0.91	1.34	0.24	67
3	0.94	1.58	0.24	59

Circulation and Drillstring Slamming

Table 5.7 contains the results of the test runs with drillstring slamming. Although these test indicate that drillstring slamming is significantly less effective than drillstring rotation it seems to be more effective than circulation alone. When factoring in the discrepancy in the initial amount of cuttings compared to table 5.5 drillstring slamming seems even more advantageous. In the equivalent test with water the improved hole cleaning effect was attributed to the occasionally positively eccentric drillstring placement causing the local flow velocity to increase in the vicinity of the cuttings bed, and thereby improve cuttings transport. During the test runs with the xanthan gum fluid, however, there was no visual observations that suggested that that was the case. On the contrary, it was observed that sand particles were being dislodged and brought into suspension by the impact of each drillstring slam.

Table 5.7: Hole cleaning results, circulating water with 0.2 wt-% xanthan gum at 60 lpm and slamming the drillstring at 5 second intervals for 4 minutes. $W_{cuttings_{test}}$ is the weight of cuttings removed after each test run. $W_{cuttings_i}$ is the initial weight of the cuttings in the test tube at the start of each run. Max $\Delta W_{cuttings_i}$ is the maximum difference in the initial amount of cuttings for the test.

Run	$W_{cuttings_{test}}$[kg]	$W_{cuttings_i}$[kg]	$Max\Delta W_{cuttings_i}$[kg]	Effectiveness[%]
1	0.09	1.05	0.30	8
2	0.19	1.35	0.30	14
3	0.26	1.33	0.30	20

Circulation, Drillstring Rotation and drillstring Slamming

Table 5.8 contains the results of the test runs combinding drillstring rotation and drillstring slamming. The results indicate that the combination of rotation and slamming is the most effective out of tests conducted. However, it is only marginally more effective than drillstring rotation alone. It is also worth noting that the initial amount of cuttings were a little higher during these tests compared to the runs with drillstring rotation alone. In contrast to the test runs with water, the combination of drillstring rotation and drillstring slamming does not seem to have a negative impact on hole cleaning compared to rotation and slamming individually.

Table 5.8: Hole cleaning results, circulating water with 0.2 wt-% xanthan gum at 60 lpm with drillstring rotation of 150 RPM and slamming the drillstring at 5 second intervals for 4 minutes. $W_{cuttings_{test}}$ is the weight of cuttings removed after each test run. $W_{cuttings_i}$ is the initial weight of the cuttings in the test tube at the start of each run. Max $\Delta W_{cuttings_i}$ is the maximum difference in the initial amount of cuttings for the test.

Run	$W_{cuttings_{test}}$[kg]	$W_{cuttings_i}$[kg]	$Max\Delta W_{cuttings_i}$[kg]	Effectiveness[%]
1	1.27	1.89	0.15	67
2	1.19	1.74	0.15	68
3	1.11	1.77	0.15	63

Chapter 6

Conclusion

As part of this thesis work a redesigned cuttings feeding system has been implemented on the existing student flow loop at the Department of Geoscience and Petroleum at NTNU. The implementation has been successfully completed, and the experiments detailed in this thesis have proven that the feeding system is capable of producing consistent results. There are still some variation in the amount of cuttings that enters the annular space during loading runs. However, the test results are significantly more consistent than with the old flow loop setup. Additionally, the current flow loop setup has shown that it is capable of producing a fairly uniform cuttings bed height which is key if one would like to compare the flow loop results to a computational fluid dynamics model.

In this study, the hole cleaning potential of drillstring slamming has been evaluated, and compared to annular flow, drillstring rotation and drillstring rotation in combination with drillstring slamming. The hole cleaning study was conducted using tap water, and a xanthan gum fluid.

The tests using water showed that annular flow rate dominates hole cleaning. The test results of drillstring slamming while circulating water yielded fantastic results. However, it was observed that cuttings transport accelerated when the drillstring moved to a positively eccentric position. This indicates that the improved hole cleaning is a result of the periodically positively eccentric drillstring, which causes the flow velocity in the vicinity of the cuttings bed to increase, rather than the slamming itself. Rotation seems to have little to no effect on hole cleaning due to the low viscosity of water.

During loading the equilibrium bed height was significantly reduced when using the xanthan gum fluid. This was attributed to the increased effect of drillstring rotation due to the higher viscosity of the xanthan gum fluid in addition to the flatter velocity profile of xanthan gum fluids in annular flow. Drillstring rotation proved superior hole cleaning effects during test runs as well. Drillstring slamming was found significantly less effective than drillstring rotation. However, it seems to be slightly more effective than circulation alone.

It was also found to not have a negative impact in combination with drillstring rotation.

Chapter 7

Further work

The linear motors used to adjust drillstring eccentricity should be improved to avoid failures and thereby improve the consistency of test results. The experiments given in the original experiment plan available in appendix A.1 should be conducted. The effects of drillstring rotation and drillstring slamming at different drillstring eccentricities and inclinations is of particular interest. Future testing should also involve the 80 wt-% glycerol fluid discussed in chapter 3.2 in order to avoid viscoelastic effects. A comparison of the glycerol fluid and the xanthan gum fluid would help identify the impact of viscoelasticity on cuttings bed buildup and cuttings transport. A study of the discrepancies encountered when loading cuttings using xanthan gum would benefit future testing.

Bibliography

Bjørn A. Brechan, e.a., 2017. Compendium: Drilling, Completion, Intervention and P&A - Design and Operation. NTNU, Department of Petroleum Engineering and Applied Geophysics.

Haugan, O.K., 2019. Influence of Drilling Parameters on Cuttings Transport. Master's thesis.

igem.org/FluidDynamics, 2018. Fluid dynamics. URL: http://2018.igem.org/Team:Queens_Canada/Fluid_Dynamics.

IHSMarkit, 2019. URL: https://ihsmarkit.com/products/oil-gas-drilling-rigs-offshore-day-rates.html.

Mingquin Duan, e.a., 2009. Critical condition for effective sand-sized-solids trasport in horizontal and high-angle wells .

Okrajni, S.S., Azar, J., 1986. The effects of mud rheology on annular hole cleaning in directional wells .

Sandahl, B.T., 2019. Drillstring manipulation to improve hole cleaning. Semester Project .

Sandahl, B.T., Sørgård, C., 2019. Rheology report .

Sayindla, S., 2018. Study of Cuttings Transport Using Water-Based and Oil-Based Drilling Fluids. Ph.D. thesis.

Sifferman, T., Becker, T., 1992. Hole cleaning in full-scale inclined wellbores .

wikipedia/viscosity, 2019. Viscosity. URL: https://en.wikipedia.org/wiki/Viscosity#/media/File:Viscous_regimes_chart.png.

Yunus A. Cengel, J.M.C., 2010. Fluid Mechanics: Fundamentals and Applications. McGraw Hill.

Appendices

Appendix A

Appendix A

A.1 Original Experiment Plan

Every experiment is conducted at 60° and 45° inclination, and is conducted using both tap water and the 80 wt-% glycerol fluid. Every experiment is run at a pump frequency of 26 Hz corresponding to approximately 60 lpm. Table 4.2 contains the linear motor settings used to achieve the drillstring slamming effect. The experiments are as follows:

- Concentric drillstring, no drillstring rotation, no lateral drillstring movement
- Positively eccentric drillstring, no drillstring rotation, no lateral drillstring movement
- Negatively eccentric drillstring, no drillstring rotation, no lateral drillstring movement

- Concentric drillstring, 150 RPM drillstring rotation, no lateral drillstring movement
- Positively eccentric drillstring, 150 RPM drillstring rotation, no lateral drillstring movement
- Negatively eccentric drillstring, 150 RPM drillstring rotation, no lateral drillstring movement

- Concentric drillstring, no drillstring rotation, lateral drillstring movement at 5 second intervals
- Positively eccentric drillstring, no drillstring rotation, lateral drillstring movement at 5 second intervals
- Negatively eccentric drillstring, no drillstring rotation, lateral drillstring movement at 5 second intervals

- Concentric drillstring, 150 RPM drillstring rotation, lateral drillstring movement at 5 second intervals
- Positively eccentric drillstring, 150 RPM drillstring rotation, lateral drillstring movement at 5 second intervals
- Negatively eccentric drillstring, 150 RPM drillstring rotation, lateral drillstring movement at 5 second intervals

Appendix B

Appendix B

B.1 HSE During Experimental Work

It is important to consider HSE in any experimental work. In order to gain access to the labs and facilities employed in the work related to this thesis several HSE-courses had to be completed. In addition to the theoretical courses, a walkthrough was completed for each lab and location involved in the thesis work. These walkthroughs included the locations of safety equipment, such as fire extinguishers and eye washing stations, in addition to emergency exits and personal protection equipment(PPE). There was also given a thorough introduction to all equipment employed by the person in charge of the given equipment. These introductions consisted of instructions on how to safely operate the equipment including necessary PPE. There was two activities that required consideration:

- Operating the flow loop
- Mixing of the xanthan gum fluid

Operating the Flow Loop

The primary risk when operating the flow loop is sprays and leaks of the slurry. However, the maximum pump outlet pressure is only about one 1.9 bar. The most likely source of sprays is the outlet tube marked as 11 in figure 4.2. At that point the pressure will have diminished due to pressure loss throughout the system. None the less, safety goggles should be worn whenever the flow loop is running.

Mixing of the Xanthan Gum Fluid

Xanthan gum is a non-toxic and non-irritating substance. In fact, it is commonly used in food items such as dressings and sauces. However, it is an extremely light and potent thickening agent. It was therefore decided that a dust mask and safety goggles should be worn when mixing the xanthan gum fluid to avoid inhaling xanthan gum dust, as inhaling xanthan gum dust may cause some respiratory discomfort.

NTNU

Norwegian University of
Science and Technology